

Original Research

# Dynamic Profiling of Exosomal microRNAs in Blood Plasma of Patients with Castration-Resistant Prostate Cancer

Elena A. Pudova<sup>1,\*</sup>, Anastasiya A. Kobelyatskaya<sup>1</sup>, Irina V. Katunina<sup>1</sup>,  
Anastasiya V. Snezhkina<sup>1</sup>, Maria S. Fedorova<sup>1</sup>, Zulfiya G. Guvatova<sup>1</sup>, Kirill M. Nyushko<sup>2</sup>,  
Boris Y. Alekseev<sup>2</sup>, Vladislav S. Pavlov<sup>1</sup>, Maria V. Savvateeva<sup>1</sup>, Alexander A. Kudryavtsev<sup>1</sup>,  
George S. Krasnov<sup>1</sup>, Anna V. Kudryavtseva<sup>1</sup>

<sup>1</sup>Engelhardt Institute of Molecular Biology, Russian Academy of Sciences, 119991 Moscow, Russia

<sup>2</sup>National Medical Research Radiological Center, Ministry of Health of the Russian Federation, 125284 Moscow, Russia

\*Correspondence: [pudova\\_elena@inbox.ru](mailto:pudova_elena@inbox.ru) (Elena A. Pudova)

Academic Editors: Poggi Alessandro and Neven Zarkovic

Submitted: 28 February 2022 Revised: 1 April 2022 Accepted: 8 April 2022 Published: 23 May 2022

## Abstract

Prostate cancer is one of the most common and socially significant cancers among men. The aim of this study was to identify significant changes in the expression of exosomal miRNAs associated with an increase in the level of prostate specific antigen in castration-resistant prostate cancer during therapy and to evaluate them as potential prognostic markers for this category of disease. High-throughput miRNA sequencing was performed on 49 blood plasma samples taken from 11 Russian patients with castration-resistant cancer during therapy. Bioinformatic analysis of the obtained miRNA-seq data was carried out. Additionally, miRNA-seq data from the PRJNA562276 project were analyzed to identify exosomal miRNAs associated with castration-resistant prostate cancer. We found 34 differentially expressed miRNAs associated with the progression of castration-resistant prostate cancer during therapy in Russian patients. It was also shown that hsa-miRNA-148a-3p expression can serve as a potential prognostic marker. We found the exosomal miRNA expression signature associated with castration-resistant prostate cancer progression, in particular on the Russian patient cohort. Many of these miRNAs are well-known players in either oncogenic transformation or tumor suppression. Further experimental studies with extended sampling are required to validate these results.

**Keywords:** castration-resistant prostate cancer; exosomes; miRNAs; NGS; progression; liquid biopsy; expression

## 1. Introduction

Prostate cancer (PCa) is one of the urgent problems of modern oncology and is characterized by high incidence rates among men [1]. The main method of treatment for patients with advanced stages of PCa is androgen deprivation. However, the progression of the tumor process against the background of the castration level of testosterone after temporary stabilization is observed in most patients. These patients are moving into the category of castration-resistant prostate cancer (CRPC), which is a prognostically unfavorable form of the disease that significantly impairs the quality of life of patients.

Despite a wide range of therapeutic options, such as cytotoxic chemotherapy agents, androgen receptor blockers, immunotherapy, and radiopharmaceuticals, metastatic CRPC remains incurable [2]. In addition, patients inevitably develop resistance to therapy, which is usually diagnosed on the basis of biochemical and radiological progression, and is a serious problem in oncology.

Therapeutic resistance is expressed as a decrease in the effectiveness and ability of drugs to have a therapeutic effect, which is one of the key problems in cancer treatment [3]. Acquired drug resistance is a stepwise process during

which significant molecular genetic events occur in tumor cells, resulting in the formation of a drug-resistant phenotype [4].

Thus, informative markers of response to therapy are needed to identify the initial manifestations of resistance to ongoing therapy and timely change the therapeutic approach for the patient. Currently, a promising direction for monitoring response to therapy in patients with predominant stages of various types of cancer is the search for biomarkers based on minimally invasive liquid biopsy [5–7]. Exosomes found in various biological fluids are of particular interest as a source of potential markers of liquid biopsy.

Exosomes are extracellular vesicles approximately 40–160 nm in size (~100 nm on average) composed of a lipid bilayer membrane that surrounds a small portion of the cytosolic content but does not include any cytoplasmic organelles [8]. Numerous studies have shown that exosomes can carry various functional molecules, including proteins, lipids, and nucleic acids (DNA, mRNA, lncRNA, microRNA, etc.) obtained from the parent cell [9]. In the case of tumor cells, exosomes can potentially reflect the molecular genetic features of the tumor [10].



**Table 1. Clinicopathological characteristics of Russian patients with CRPC.**

Patients	Age	Gleason score	PSA at diagnosis, ng/mL	Therapy	Radionuclide study of the skeletal system
1	66	9 (5 + 4)	3000	Docetaxel	multiple bone metastasis
2	68	8 (4 + 4)	1900	Docetaxel	bone metastasis
3	66	-	5	Abiraterone	bone metastasis
4	65	-	428	Abiraterone	bone metastasis
5	61	8 (4 + 4)	23	Docetaxel	multiple bone metastasis
6	68	8 (4 + 4)	124	Docetaxel	bone metastasis
7	70	8 (4 + 4)	72	Docetaxel	bone metastasis
8	73	8 (4 + 4)	2950	Docetaxel	bone metastasis
9	66	8 (4 + 4)	334	Docetaxel	bone metastasis
10	67	9 (4 + 5)	25	Abiraterone	bone metastasis
11	61	7 (4 + 3)	15	Abiraterone	bone metastasis

Exosomes play an important role in the regulation of intercellular interaction, including due to the protection of their contents from environmental conditions, which emphasizes their attractiveness for research [11]. An increased number of exosomes is usually secreted by tumor cells, often correlating between the stage of the disease and its progression. These vesicles mediate intercellular communication and perform important functions in tumor biology, such as proliferation induction, angiogenesis, and metastasis [12–14]. Recently, there has been a growing body of evidence highlighting the important role of exosomes in modulating tumor-specific chemoresistance strategies that lead to the induction of tumor drug resistance [15–17]. It has been shown that exosomes from chemosensitive/resistant tumor cells can markedly influence other tumor cells during chemotherapy through the transfer of specific regulatory molecules [18].

Thus, there are a number of fundamental questions about the molecular basis of tumor resistance to various drugs. The aim of our study is to identify the profile of exosomal miRNAs in the blood plasma of Russian patients with CRPC associated with initial manifestations of therapy resistance. Evaluation of the prognostic potential of these molecules, as well as consideration of potential therapeutic targets based on key molecular events, is especially important for predicting therapeutic efficacy/resistance to therapy, patient prognosis, and the development of precision cancer medicine.

## 2. Materials and Methods

### 2.1 Materials

The study included 49 plasma samples from 11 Russian patients with metastatic CRPC during therapy (docetaxel/abiraterone), obtained under observation in the P.A. Herten Moscow Oncology Research Center (branch of the National Medical Research Radiological Center, Ministry of Health of the Russian Federation) in 2016–2020. The main clinicopathological characteristics of patients are presented in Table 1.

To create a collection of exosomal RNA, blood was

taken into EDTA vacutainers, which were then subjected to double centrifugation at 4 °C (the first step of centrifugation –20 minutes at 300 g, the second step of centrifugation –10 minutes at 14,000 g) followed by storage at –80 °C.

All plasma samples were tested for hemolysis by color scoring according to the metric hemolysis score on the color scale. Hemolysis was also assessed by measuring free hemoglobin uptake in samples at 414 nm using a NanoDrop™ 1000 spectrophotometer (Thermo Scientific, USA).

The studied samples were divided into several conditional groups during the observation process in accordance with the dynamics of the prostate specific antigen (PSA) level in each patient during treatment: period P0—start of therapy, period P1—response to therapy (stable low PSA level of the patient), period P2—(patient’s initial increase in PSA level), period P3—(elevated PSA level in a patient).

The study also analyzed exosomal miRNAs profiling data from the PRJNA562276 project (treatment-naïve PCA patients  $n = 24$ , CRPC patients  $n = 24$ ) to confirm the involvement of certain circulating miRNAs in the CRPC category [19].

### 2.2 Methods

#### 2.2.1 Determination of PSA Level Concentration in Samples

To assess the dynamics of response to therapy in patients with CRPC, an enzyme-linked immunosorbent assay for the concentration of PSA in each blood plasma sample was performed using the “total PSA—option 1” reagent kit (Vector-Best, Russia). The assay was performed in three technical replicates according to the manufacturer’s protocol. The registration of the obtained results was carried out on an iMark™ Microplate Absorbance Reader spectrophotometer (BioRad, USA) at a main wavelength of 450 nm and a reference wavelength in the range of 620–655 nm.

#### 2.2.2 Isolation of Total Exosomal RNA

Blood plasma samples were subjected to additional purification through specialized filters with a pore size

of 0.8  $\mu\text{m}$  (Sartorius, Germany). Isolation of total exosomal RNA was performed from 1 mL of filtered blood plasma using the exoRNeasy Serum-Plasma Midi Kit (Qiagen, Germany) according to the manufacturer's protocol. This methodology involves the use of specialized affinity membrane spin columns to efficiently capture exosomes and other extracellular vesicles from various biological fluids [20,21].

During RNA isolation, cel-miR-39 (Norgene, Canada) was added to each sample as a normalization control according to the manufacturer's protocol. The concentration of isolated total RNA was assessed on a Qubit 4.0 fluorimeter (Thermo Fisher Scientific, USA) using the Qubit microRNA Assay Kit (Thermo Fisher Scientific, USA).

### 2.2.3 Preparation of miRNAs Libraries

miRNAs libraries were prepared using the NEBNext Small RNA Library Prep Set for Illumina (New England Biolabs, USA) according to the manufacturer's protocol. Selection of the miRNA fraction was carried out using electrophoretic separation of fragments in a 6% polyacrylamide gel, followed by extraction and concentration in accordance with the manufacturer's protocol.

The concentration of the resulting libraries was measured on a Qubit 4.0 fluorimeter using the Qubit dsDNA HS Assay Kit (Thermo Fisher Scientific, USA). The quality of the resulting libraries was assessed on an Agilent Bioanalyzer 2100 instrument using the Agilent High Sensitivity DNA Kit (Thermo Fisher Scientific, USA) in accordance with the manufacturer's protocol. The size of the resulting miRNA libraries was  $\sim 147$  bp.

### 2.2.4 Next Generation Sequencing (NGS)

High throughput sequencing of miRNA libraries was performed on a NextSeq 500 System (Illumina) using NextSeq 500/550 High Output Kit v2.5 (Illumina) in 36 bp single-ended read mode. Sequencing was carried out on the basis of the Center for Collective Use "Genome" of the EIMB RAS ([http://www.eimb.ru/ru1/ckp/ccu\\_genome\\_c.php](http://www.eimb.ru/ru1/ckp/ccu_genome_c.php)). As a result of the sequencing for each sample, at least 8 million reads were obtained.

### 2.2.5 miRNA-Seq Data Analysis

For the obtained miRNA-seq data in the fastq format, the quality was assessed using the FastQC and MultiQC programs (<https://www.bioinformatics.babraham.ac.uk/projects/fastqc/>). The miRge 2.0 pipeline was used for data processing [22]. Data on the number of obtained transcripts miRNA (counts) were obtained using the featureCounts [23].

Differential miRNA expression analysis was performed in the R statistical environment using the edgeR package [24]. To normalize the data, the TMM (Trimmed

Mean of M-values) method was used, followed by the calculation of the CPM (counts per million) parameter. When analyzing the differential expression of miRNAs, the following quasi-likelihood F-test (QLF test), Wilcoxon test (W test) for comparisons in paired mode were applied. Spearman's rank correlation coefficient ( $r_s$ ) was used for correlation analysis of the data. Differences in miRNA expression levels were considered statistically significant at test  $p$ -values  $< 0.05$ .

To analyze the enrichment of pathways based on miRNA-Seq data, the mirPath 3.0 tool of the DIANA Tools web service was used [25]. The results obtained were considered significant at  $p$ -value  $< 0.01$ .

Survival analysis using the Cox regression model was performed with Jupyter Notebook, Python (ver. 3.6), native libraries and 'Lifelines' library (Kaplan-Meier, COX). Results were presented as hazard ratio (HR) and 95% confidence intervals (CI) and were considered significant at  $p < 0.05$ .

### 2.2.6 Quantitative Polymerase Chain Reaction (qPCR)

cDNA was obtained from the miRNA template using the TaqMan Advanced miRNA cDNA Synthesis Kit (Thermo Fisher Scientific, USA) according to the manufacturer's protocol.

qPCR was carried out in three technical repeats on an Applied Biosystems 7500 instrument (Thermo Fisher Scientific, USA). cel-miR-39 served as a reference miRNA. For the detection of control and target miRNAs, commercial sets of primers and probes TaqMan<sup>TM</sup> Advanced miRNA Assay (Thermo Fisher Scientific, USA) were used: 477814\_mir (miR-148a-3p), 478293\_mir (cel-miR-39).

The level of relative miRNA expression for each study period was calculated by the dCT method. Statistical analysis of relative miRNA results was performed in the R statistical environment using standard packages.

## 3. Results

### 3.1 Differentially Expressed Exosomal miRNAs Associated with CRPC

First of all, we analyzed the differential expression (DE) of exosomal miRNAs between the P1 and P3 periods during CRPC therapy. The statistical significance level of the QLF, W and  $r_s$  tests ( $p < 0.05$ ) was used as key parameters for filtering the results. As a result, we received a list of 34 microRNAs with the specified criteria (Table 2, Fig. 1).

DE exosomal miRNAs were then analyzed between the remaining periods of CRPC therapy. The level of statistical significance for QLF, W and  $r_s$  tests ( $p < 0.05$ ) was also used as the main parameters for filtering the results. As a result of DE analysis between the P0 and P3 periods, we received a list of 7 miRNAs with the specified criteria (Table 3, Fig. 2A).

**Table 2. List of differentially expressed exosomal miRNAs between the P1 and P3 periods in Russian patients with CRPC during therapy.**

miRs	LogFC	LogCPM	$p$ (QLF)	$p$ (W)	$r_s$	$p$ ( $r_s$ )
hsa-let-7f-5p	-1.34	15.02	$3.03 \times 10^{-3}$	$9.77 \times 10^{-4}$	-0.64	$1.41 \times 10^{-3}$
hsa-let-7g-5p	-1.80	13.96	$2.07 \times 10^{-4}$	$9.77 \times 10^{-4}$	-0.72	$1.41 \times 10^{-4}$
hsa-miR-1-3p	-2.73	12.01	$9.69 \times 10^{-5}$	$9.77 \times 10^{-3}$	-0.42	$4.99 \times 10^{-2}$
hsa-miR-122-5p	2.71	11.85	$6.78 \times 10^{-5}$	$4.88 \times 10^{-3}$	0.71	$2.19 \times 10^{-4}$
hsa-miR-125b-1-3p	-9.24	9.10	$1.55 \times 10^{-7}$	$3.46 \times 10^{-2}$	-0.46	$3.20 \times 10^{-2}$
hsa-miR-125b-2-3p	-3.20	10.07	$2.35 \times 10^{-3}$	$9.77 \times 10^{-3}$	-0.43	$4.75 \times 10^{-2}$
hsa-miR-126-3p	1.16	14.48	$1.23 \times 10^{-2}$	$3.22 \times 10^{-2}$	0.54	$9.91 \times 10^{-3}$
hsa-miR-1275	-5.41	5.15	$3.94 \times 10^{-2}$	$2.25 \times 10^{-2}$	-0.52	$1.24 \times 10^{-2}$
hsa-miR-1307-3p	1.75	10.05	$1.15 \times 10^{-2}$	$9.77 \times 10^{-4}$	0.74	$8.85 \times 10^{-5}$
hsa-miR-132-3p	-7.20	7.04	$1.49 \times 10^{-3}$	$1.91 \times 10^{-2}$	-0.45	$3.44 \times 10^{-2}$
hsa-miR-132-5p	-7.53	5.45	$9.23 \times 10^{-3}$	$2.09 \times 10^{-2}$	-0.65	$1.03 \times 10^{-3}$
hsa-miR-143-3p	-2.74	18.35	$3.31 \times 10^{-8}$	$6.84 \times 10^{-3}$	-0.48	$2.38 \times 10^{-2}$
hsa-miR-145-3p	-2.45	9.01	$1.58 \times 10^{-2}$	$8.05 \times 10^{-3}$	-0.43	$4.86 \times 10^{-2}$
hsa-miR-148a-3p	-2.49	18.26	$9.02 \times 10^{-9}$	$9.77 \times 10^{-4}$	-0.75	$5.38 \times 10^{-5}$
hsa-miR-148b-3p	-1.83	11.25	$3.22 \times 10^{-3}$	$9.77 \times 10^{-4}$	-0.77	$3.17 \times 10^{-5}$
hsa-miR-152-3p	-2.46	10.49	$8.48 \times 10^{-4}$	$9.77 \times 10^{-4}$	-0.61	$2.62 \times 10^{-3}$
hsa-miR-185-3p	-9.01	7.06	$1.50 \times 10^{-5}$	$9.15 \times 10^{-3}$	-0.68	$4.89 \times 10^{-4}$
hsa-miR-21-3p	-7.53	5.27	$5.55 \times 10^{-3}$	$2.25 \times 10^{-2}$	-0.67	$6.95 \times 10^{-4}$
hsa-miR-221-5p	-6.82	5.36	$2.98 \times 10^{-2}$	$8.05 \times 10^{-3}$	-0.72	$1.59 \times 10^{-4}$
hsa-miR-23a-3p/23b-3p	-1.79	11.60	$2.71 \times 10^{-3}$	$9.77 \times 10^{-4}$	-0.74	$8.85 \times 10^{-5}$
hsa-miR-27a-3p/27b-3p	-1.27	13.67	$9.18 \times 10^{-3}$	$9.77 \times 10^{-4}$	-0.61	$2.63 \times 10^{-3}$
hsa-miR-29b-3p	-6.95	5.95	$1.18 \times 10^{-2}$	$5.92 \times 10^{-3}$	-0.72	$1.59 \times 10^{-4}$
hsa-miR-30e-3p	-1.43	11.40	$2.84 \times 10^{-2}$	$1.37 \times 10^{-2}$	-0.45	$3.49 \times 10^{-2}$
hsa-miR-320a-3p	1.81	11.96	$1.29 \times 10^{-3}$	$1.95 \times 10^{-3}$	0.75	$5.38 \times 10^{-5}$
hsa-miR-342-5p	1.75	9.35	$3.64 \times 10^{-2}$	$9.77 \times 10^{-4}$	0.62	$1.94 \times 10^{-3}$
hsa-miR-378a-3p	-2.14	12.28	$7.18 \times 10^{-4}$	$1.37 \times 10^{-2}$	-0.55	$7.78 \times 10^{-3}$
hsa-miR-423-5p	2.37	13.54	$4.51 \times 10^{-6}$	$9.77 \times 10^{-4}$	0.69	$3.31 \times 10^{-4}$
hsa-miR-424-3p	6.50	6.06	$2.58 \times 10^{-2}$	$1.29 \times 10^{-2}$	0.57	$5.20 \times 10^{-3}$
hsa-miR-4446-3p	4.15	7.33	$1.55 \times 10^{-2}$	$9.15 \times 10^{-3}$	0.61	$2.61 \times 10^{-3}$
hsa-miR-483-5p	4.68	7.47	$1.10 \times 10^{-2}$	$8.05 \times 10^{-3}$	0.58	$5.10 \times 10^{-3}$
hsa-miR-574-5p	-7.16	7.73	$1.07 \times 10^{-3}$	$8.05 \times 10^{-3}$	-0.59	$4.06 \times 10^{-3}$
hsa-miR-582-3p	-7.65	7.94	$1.72 \times 10^{-5}$	$1.95 \times 10^{-3}$	-0.71	$2.40 \times 10^{-4}$
hsa-miR-744-5p	1.77	10.10	$1.04 \times 10^{-2}$	$9.77 \times 10^{-4}$	0.59	$3.51 \times 10^{-3}$
hsa-miR-9-5p	-7.11	6.78	$4.76 \times 10^{-3}$	$9.15 \times 10^{-3}$	-0.58	$4.72 \times 10^{-3}$

**Table 3. List of differentially expressed exosomal miRNAs between the P0 and P3 periods in Russian patients with CRPC during therapy.**

miRs	LogFC	LogCPM	$p$ (QLF)	$p$ (W)	$r_s$	$p$ ( $r_s$ )
hsa-let-7g-5p	-0.37	13.9	$3.41 \times 10^{-2}$	$2.44 \times 10^{-2}$	-0.57	$6.04 \times 10^{-3}$
hsa-miR-148a-3p	-0.44	17.93	$2.42 \times 10^{-3}$	$4.37 \times 10^{-2}$	-0.47	$2.89 \times 10^{-2}$
hsa-miR-122-5p	0.7	12.25	$1.55 \times 10^{-3}$	$1.37 \times 10^{-2}$	0.55	$7.78 \times 10^{-3}$
hsa-miR-193a-5p	2.83	6.92	$6.96 \times 10^{-4}$	$2.09 \times 10^{-2}$	0.64	$1.50 \times 10^{-3}$
hsa-miR-320a-3p	0.57	12.5	$6.19 \times 10^{-3}$	$2.44 \times 10^{-2}$	0.51	$1.56 \times 10^{-2}$
hsa-miR-342-5p	0.6	9.69	$3.99 \times 10^{-2}$	$9.77 \times 10^{-3}$	0.62	$1.94 \times 10^{-3}$
hsa-miR-423-5p	0.47	14.09	$7.76 \times 10^{-3}$	$3.22 \times 10^{-2}$	0.47	$2.89 \times 10^{-2}$

As a result of the DE analysis between P1 and P2 periods, 15 statistically significant miRNAs were identified (Table 4, Fig. 2B). However, in the case of DE analysis between P2 and P3 periods, a statistically significant result was obtained only for hsa-miR-423-5p (LogFC = 0.66; LogCPM = 14.38;  $p$  (QLF) =  $3.49 \times 10^{-2}$ ;  $p$  (W) =  $3.60 \times$

$10^{-2}$ ). The result of the correlation analysis for this miRNA did not pass the threshold of statistical significance ( $r_s = 0.23$ ;  $p$  ( $r_s$ ) =  $3.04 \times 10^{-1}$ ).

Additionally, we analyzed the data of the PR-JNA562276 project, in the analysis of which the level of statistical significance for QLF, and  $r_s$  tests ( $p < 0.05$ ) was

**Table 4. List of differentially expressed exosomal miRNAs between the P1 and P2 periods in Russian patients with CRPC during therapy.**

miRs	LogFC	LogCPM	$p$ (QLF)	$p$ (W)	$r_s$	$p$ ( $r_s$ )
hsa-let-7g-5p	-1.23	13.82	$6.99 \times 10^{-3}$	$2.44 \times 10^{-2}$	-0.52	$1.25 \times 10^{-2}$
hsa-miR-122-5p	1.67	11.45	$5.36 \times 10^{-3}$	$1.37 \times 10^{-2}$	0.42	$5.00 \times 10^{-2}$
hsa-miR-132-5p	-6.13	5.31	$2.57 \times 10^{-2}$	$2.09 \times 10^{-2}$	-0.55	$8.33 \times 10^{-3}$
hsa-miR-139-3p	3.39	7.86	$8.59 \times 10^{-3}$	$9.77 \times 10^{-3}$	0.57	$5.69 \times 10^{-3}$
hsa-miR-148a-3p	-1.71	18.34	$3.14 \times 10^{-5}$	$4.20 \times 10^{-2}$	-0.49	$1.94 \times 10^{-2}$
hsa-miR-148b-3p	-1.4	11.2	$1.95 \times 10^{-2}$	$2.44 \times 10^{-2}$	-0.58	$4.63 \times 10^{-3}$
hsa-miR-185-3p	-8.93	7.15	$1.22 \times 10^{-6}$	$9.15 \times 10^{-3}$	-0.67	$7.33 \times 10^{-4}$
hsa-miR-21-3p	-4.85	5.23	$4.50 \times 10^{-2}$	$2.25 \times 10^{-2}$	-0.49	$2.05 \times 10^{-2}$
hsa-miR-23a-3p/23b-3p	-1.38	11.47	$1.76 \times 10^{-2}$	$2.44 \times 10^{-2}$	-0.51	$1.56 \times 10^{-2}$
hsa-miR-320a-3p	1.41	11.66	$1.26 \times 10^{-2}$	$3.22 \times 10^{-2}$	0.51	$1.56 \times 10^{-2}$
hsa-miR-330-5p	-4.71	4.92	$4.39 \times 10^{-2}$	$3.60 \times 10^{-2}$	-0.48	$2.50 \times 10^{-2}$
hsa-miR-423-5p	1.51	12.96	$2.72 \times 10^{-3}$	$9.77 \times 10^{-4}$	0.55	$7.78 \times 10^{-3}$
hsa-miR-483-5p	4.32	7.09	$2.81 \times 10^{-2}$	$2.49 \times 10^{-2}$	0.44	$4.02 \times 10^{-2}$
hsa-miR-548a-3p	-4.71	6.09	$2.23 \times 10^{-2}$	$1.29 \times 10^{-2}$	-0.54	$9.22 \times 10^{-3}$
hsa-miR-582-3p	-3.49	8.21	$1.19 \times 10^{-2}$	$1.37 \times 10^{-2}$	-0.55	$7.36 \times 10^{-3}$

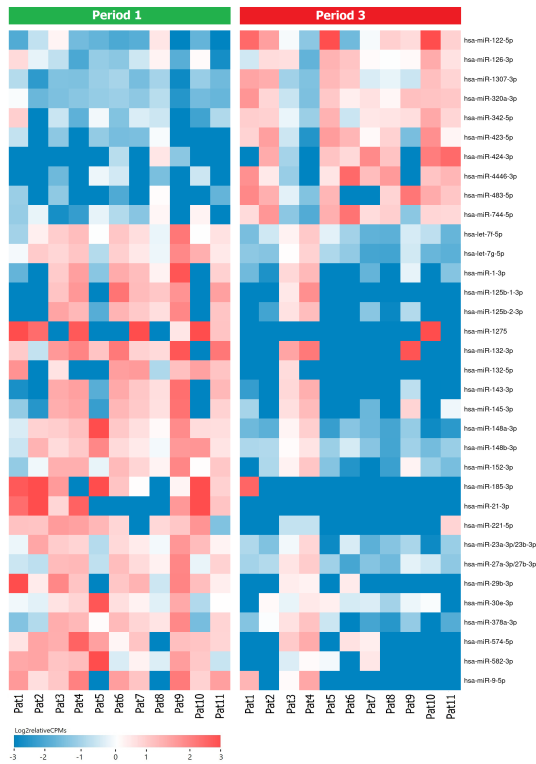


**Fig. 1. Heatmap demonstrating log relative expression level of top differentially expressed exosomal miRNAs between the P1 and P3 periods.** Cell colors (blue-white-red gradient) correspond to the binary logarithm of the ratio of the expression level in a current sample to the average level across all the samples (per each miRNA). Blue, expression level is below the average; red, above the average.

used as key parameters for filtering the results. As a result, we obtained a list of 11 miRNAs that meet the specified criteria (Table 5).

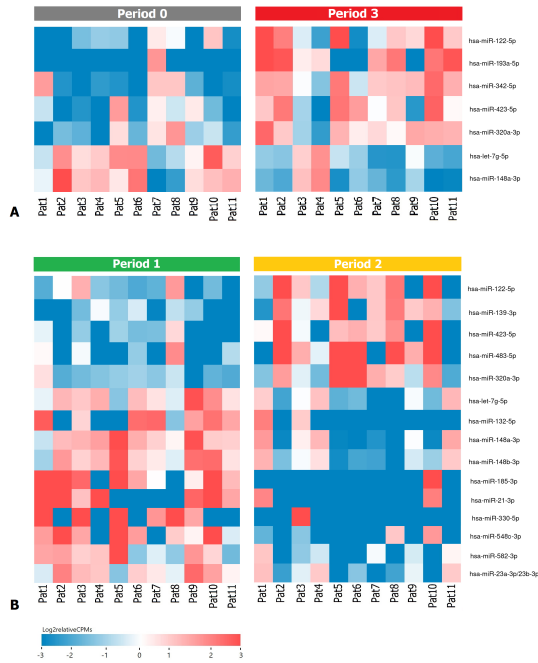
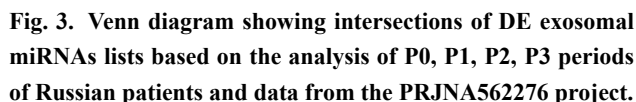


**Fig. 2. Heatmap demonstrating log relative expression level of top differentially expressed exosomal miRNAs (A) between the P0 and P3 periods (B) between the P1 and P2 periods.** Cell colors (blue-white-red gradient) correspond to the binary logarithm of the ratio of the expression level in a current sample to the average level across all the samples (per each miRNA). Blue, expression level is below the average; red, above the average.

When considering all the obtained lists of DE exosomal miRNAs, we see that hsa-miR-148a-3p and hsa-miR-320a-3p were found in all. Moreover, the expression of these miRNAs is presented at a high level (LogCPM > 11), which indicates a possible key role of these molecules in the development and progression of CRPC (Fig. 3).

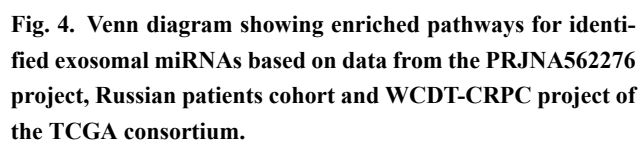


miRs	LogFC	LogCPM	$p$ (QLF)	$r_s$	$p$ ( $r_s$ )
hsa-miR-375-3p	3.82	12.0	$6.68 \times 10^{-6}$	0.50	$3.00 \times 10^{-4}$
hsa-miR-99a-5p	0.81	13.0	$2.00 \times 10^{-4}$	0.45	$2.00 \times 10^{-3}$
hsa-miR-1246	2.49	10.7	$1.00 \times 10^{-3}$	0.39	$7.00 \times 10^{-3}$
hsa-miR-148a-3p	0.91	14.9	$2.00 \times 10^{-4}$	0.36	$1.00 \times 10^{-2}$
hsa-miR-320a-3p	0.65	14.6	$2.00 \times 10^{-3}$	0.38	$8.00 \times 10^{-3}$
hsa-miR-30d-5p	0.57	14.1	$7.00 \times 10^{-4}$	0.38	$8.00 \times 10^{-3}$
hsa-miR-423-3p	0.71	12.3	$2.00 \times 10^{-2}$	0.36	$1.00 \times 10^{-2}$
hsa-miR-451a	-0.49	17.5	$4.00 \times 10^{-2}$	-0.40	$5.00 \times 10^{-3}$
hsa-miR-21-5p	0.51	14.6	$5.00 \times 10^{-3}$	0.33	$2.00 \times 10^{-2}$
hsa-let-7f-5p	0.33	14.2	$2.00 \times 10^{-2}$	0.31	$3.00 \times 10^{-2}$
hsa-miR-24-3p	0.45	12.2	$3.00 \times 10^{-2}$	0.33	$2.00 \times 10^{-2}$



Next, we performed the pathway enrichment analysis for the identified exosomal miRNAs using the KEGG (Kyoto Encyclopedia of Genes and Genomes) database and TarBase v7.0 (<http://www.microrna.gr/tarbase>) for target genes prediction. For the list of DE of exosomal miRNAs associated with the progression of CRPC during therapy (comparison between P1 and P3 periods), 29 statistically significant pathways were identified ( $p < 0.01$ ; Table 6). For the list of DE of exosomal miRNAs associated with CRPC (data of the PRJNA562276 project), 30 significant statistically significant pathways were identified ( $p < 0.01$ ; Table 7).

CRPC project of the TCGA consortium, which resulted in a list of enriched pathways whose expression of involved genes is associated with time to relapse in patients receiving therapy [26]. When comparing the results obtained for these distant metastases datasets with miRNA data, we see the intersection of the following signaling pathways: “Hippo signaling pathway”, “TGF-beta signaling pathway” and “Transcriptional dysregulation in cancer”. The results for the intersection of pathways are shown in the Fig. 4.



A Cox proportional hazards model was constructed to explore the relationship between time to progression in the patient and the expression of a number of identified miRNAs as predictor variables. Samples from patients of all considered periods (n = 49) were used for analysis. The model included the most abundant exosomal miRNAs in the samples from the previously identified profile (LogCPM  $\geq 10$ ), as well as the presence of which was present in each sample of all time periods (miRNA counts  $> 0$ ). Thus, the analysis included 9 miRNAs that corresponded to the specified parameters: hsa-let-7g-5p, hsa-miR-122-5p, hsa-miR-148a-3p, hsa-miR-23a-3p/23b-3p, hsa-let-7f-5p, hsa-miR-126-3p, hsa-miR-143-3p, hsa-miR-744-5p, hsa-miR-423-5p.

 **IMR Press**

**Table 6. List of enriched pathways for identified exosomal miRNAs associated with P3 period in Russian patients with CRPC during therapy.**

KEGG pathway	FDR	#genes	#miRNAs
Prion diseases	$4.84 \times 10^{-14}$	15	6
Fatty acid metabolism	$4.84 \times 10^{-14}$	17	9
Viral carcinogenesis	$4.84 \times 10^{-14}$	117	9
Hippo signaling pathway	$4.84 \times 10^{-14}$	82	10
ECM-receptor interaction	$4.84 \times 10^{-14}$	48	11
Fatty acid biosynthesis	$4.84 \times 10^{-14}$	5	12
Lysine degradation	$4.84 \times 10^{-14}$	31	12
Proteoglycans in cancer	$4.84 \times 10^{-14}$	137	14
Glioma	$4.84 \times 10^{-14}$	44	9
Chronic myeloid leukemia	$4.99 \times 10^{-13}$	55	8
Cell cycle	$1.76 \times 10^{-11}$	68	7
TGF-beta signaling pathway	$4.06 \times 10^{-11}$	52	8
Adherens junction	$7.89 \times 10^{-11}$	52	9
Pathways in cancer	$6.58 \times 10^{-9}$	179	5
Hepatitis B	$2.36 \times 10^{-8}$	74	5
Thyroid hormone signaling pathway	$3.12 \times 10^{-7}$	61	5
p53 signaling pathway	$4.66 \times 10^{-7}$	44	7
Steroid biosynthesis	$8.92 \times 10^{-6}$	8	6
Small cell lung cancer	$1.58 \times 10^{-5}$	55	6
FoxO signaling pathway	$1.92 \times 10^{-5}$	60	4
Transcriptional misregulation in cancer	$3.58 \times 10^{-5}$	61	5
Protein processing in endoplasmic reticulum	$8.47 \times 10^{-5}$	83	5
Bacterial invasion of epithelial cells	$2.32 \times 10^{-4}$	42	3
Colorectal cancer	$3.04 \times 10^{-4}$	30	2
Renal cell carcinoma	$8.07 \times 10^{-4}$	36	3
Central carbon metabolism in cancer	$8.12 \times 10^{-4}$	31	4
Non-small cell lung cancer	$8.77 \times 10^{-4}$	29	4
Prostate cancer	$4.45 \times 10^{-3}$	50	4
Oocyte meiosis	$6.60 \times 10^{-3}$	60	6

#, number of genes-targets (genes) or miRNAs.

### 3.4 Expression of Exosomal miR-148a-3p as a Potential Prognostic Marker in CRPC

Exosomal hsa-148a-3p was selected for validation based on statistically significant DE analysis results between periods P1/P3 (baseline comparison), periods P0/P3, P1/P2, and Cox regression analysis. The level of hsa-miR-148a-3p relative expression was assessed by qPCR in plasma samples from Russian patients between all periods under consideration.

As a result of the validation, a statistically significant difference was confirmed between the periods P1 and P3 ( $p(W) = 0.02$ ), as well as between the periods P0 and P3 ( $p(W) = 0.03$ ). No statistically significant difference was found based on the relative expression of hsa-miR-148a-3p between periods P1 and P2 ( $p(W) = 0.08$ ) (Fig. 6).

## 4. Discussion

The development of drug resistance in patients with CRPC is one of the most important clinical problems, which may be based on both genetic changes and interactions in

the tumor microenvironment [27]. miRNAs in exosomes can be key regulators of the resistance mechanism in cancer, which has been repeatedly emphasized by various studies. We first looked at enriched pathways that are potentially associated with both the development of CRPC and progression during therapy. After comparing the obtained results, including those of the WCDT-CRPC project, it was shown that the pathways ‘Hippo signaling pathway’, ‘TGF- $\beta$  signaling pathway’ and ‘Transcriptional misregulation in cancer’ have a statistically significant association with CRPC. The ‘Hippo signaling pathway’ plays an important role in stem cells and cancer biology [28,29]. It acts as a crucial regulator of cell growth and proliferation, organ development, cellular homeostasis and regeneration [30]. The ‘Hippo signaling pathway’ is regulated by a variety of signals such as cell density/polarity, mechanotransduction, nutrients, and through G-protein coupled receptors [31]. Importantly, the apparent kinase cascade-independent regulation by Yes-associated protein (YAP)/transcriptional coactivator with a PDZ-binding motif (TAZ) occupies one of

**Table 7. List of enriched pathways for identified exosomal miRNAs associated with CRPC.**

KEGG pathway	FDR	#genes	#miRNAs
Fatty acid biosynthesis	$1.11 \times 10^{-16}$	5	3
Proteoglycans in cancer	$1.11 \times 10^{-16}$	118	7
Lysine degradation	$1.11 \times 10^{-16}$	26	6
Viral carcinogenesis	$1.33 \times 10^{-15}$	105	7
Hippo signaling pathway	$1.45 \times 10^{-14}$	77	6
Pathways in cancer	$1.14 \times 10^{-12}$	160	5
Prion diseases	$9.52 \times 10^{-9}$	3	1
Chronic myeloid leukemia	$1.74 \times 10^{-8}$	39	4
Cell cycle	$3.56 \times 10^{-8}$	63	3
Colorectal cancer	$5.05 \times 10^{-8}$	27	3
Glioma	$7.44 \times 10^{-8}$	25	3
Oocyte meiosis	$1.03 \times 10^{-7}$	53	4
Hepatitis B	$1.19 \times 10^{-7}$	55	2
Thyroid hormone signaling pathway	$4.31 \times 10^{-7}$	50	3
Transcriptional misregulation in cancer	$5.22 \times 10^{-7}$	52	3
p53 signaling pathway	$1.19 \times 10^{-6}$	30	3
Fatty acid metabolism	$3.88 \times 10^{-6}$	19	3
TGF-beta signaling pathway	$4.14 \times 10^{-6}$	21	2
Adherens junction	$5.06 \times 10^{-5}$	41	4
Bladder cancer	$6.05 \times 10^{-5}$	22	3
FoxO signaling pathway	$2.09 \times 10^{-4}$	48	3
Protein processing in endoplasmic reticulum	$3.52 \times 10^{-4}$	52	2
ECM-receptor interaction	$1.51 \times 10^{-3}$	13	1
Endocytosis	$2.15 \times 10^{-3}$	59	2
Parkinson's disease	$2.65 \times 10^{-3}$	6	2
Ubiquitin mediated proteolysis	$2.84 \times 10^{-3}$	37	1
Central carbon metabolism in cancer	$3.15 \times 10^{-3}$	9	1
Pancreatic cancer	$4.41 \times 10^{-3}$	20	1
Mucin type O-Glycan biosynthesis	$6.20 \times 10^{-3}$	8	1
Thyroid cancer	$6.83 \times 10^{-3}$	9	2

#, number of genes-targets (genes) or miRNAs.

**Table 8. Results of Cox regression analysis for a model based on the expression of 9 exosomal miRNAs in Russian patients with CRPC during therapy, including four main time periods: P0, P1, P2 and P3.**

Covariate	HR	HR lower 95%	HR upper 95%	p
hsa-let-7g-5p	1.37	0.53	3.57	0.52
hsa-miR-122-5p	0.65	0.10	4.39	0.66
hsa-miR-148a-3p	2.05	1.29	3.25	0.005
hsa-miR-23a-3p/23b-3p	1.16	0.53	2.57	0.71
hsa-let-7f-5p	0.48	0.21	1.08	0.08
hsa-miR-126-3p	1.76	0.90	3.43	0.10
hsa-miR-143-3p	0.96	0.73	1.26	0.77
hsa-miR-744-5p	1.03	0.54	1.96	0.92
hsa-miR-423-5p	1.12	0.62	2.04	0.71
therapy	1.14	0.53	2.48	0.74

the key signals in the ‘Hippo signaling pathway’ [32]. Active regulation of the downstream effectors of the Hippo pathway, YAP/TAZ, is central in various solid tumors [33].

YAP has been identified as being amplified in a subset of PCa [34]. YAP and TAZ have been shown to play key roles in many stages of PCa initiation, development, and progression, as well as in the regulation of AR signaling. However, the mechanistic understanding of how YAP/TAZ becomes hyperactivated, how YAP/TAZ interacts with the stroma, and their precise role in the development of PCa is currently far from being fully elucidated [35].

TGF- $\beta$  plays an important role in the progression of PCa. It acts as a tumor suppressor in the early stages of epithelial cancer by inhibiting proliferation and inducing apoptosis [36]. However, in the later stages of the disease, TGF- $\beta$  acts as a tumor promoter and is associated with the development of its aggressive form [37]. The microenvironment of tumor cells plays an important role in the development and progression of the disease. Various cell types, including carcinoma-associated stromal cells, endothelial cells, lymphocytes, and tumor epithelial cells, constitute a dynamic tumor microenvironment under the regulatory control of TGF- $\beta$ , promoting tumor growth and progression



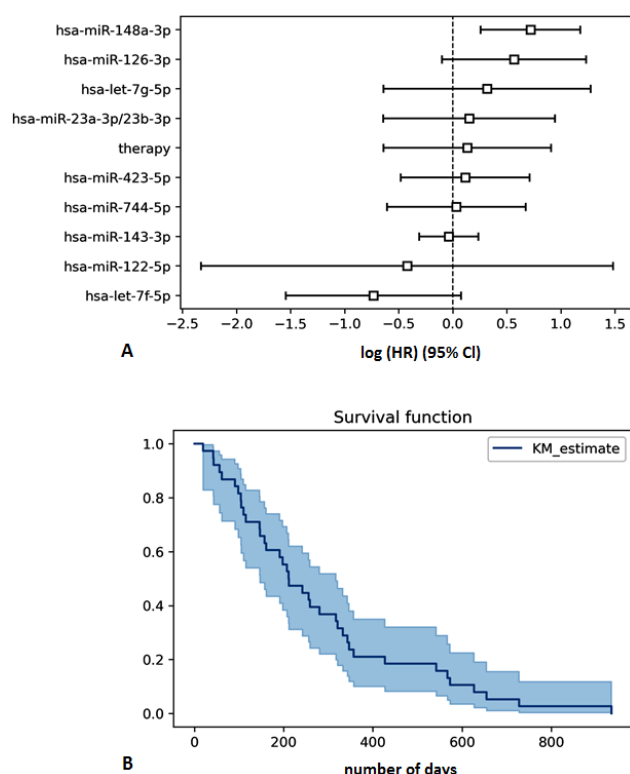


**Fig. 5. Results of survival analysis using the Cox regression model based on DE of exosomal miRNAs in the Russian patients cohort with CRPC (A) Plot of the Cox regression model covariates. Point estimates and 95% confidence intervals of the relative risks for 10 covariates in a Cox regression model of overall survival. (B) Survival curve based on the Cox regression model.**

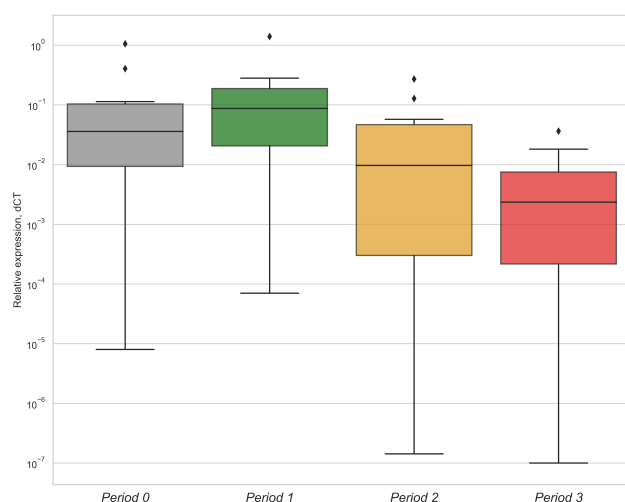


**Fig. 6. Relative expression of hsa-miR-148a-3p in plasma samples from Russian patients according to P0, P1, P2 and P3 periods based on qPCR results.**

[38]. TGF- $\beta$  plays its regulatory role in angiogenesis, invasion and migration, and the epithelial-mesenchymal transition through multiple interactions between tumor epithe-

lial cells and myofibroblasts, maintaining a reactive tumor microenvironment critical for the metastatic spread of PCa [37]. Transcriptional dysregulation leading to changes in the expression of key oncogenes is an important event responsible for the acquisition of cancer cell hallmarks such as proliferation, replicative immortality and metastasis [39].

More detailed studies of these signaling pathways and their key genes involved in the aspect of CRPC will help identify new therapeutic targets to improve the effectiveness of CRPC treatment. We also analyzed exosomal DE miRNAs as potentially significant regulators in CRPC. It is known that miRNAs are small non-coding RNAs that can play both oncogenic and tumor-suppressing roles, regularizing many cellular processes such as invasion, metastasis, apoptosis, epithelial-mesenchymal cell transition, chemoresistance, and others at the post-transcriptional level [40]. Based on the obtained differential expression parameters, statistical tests performed and survival analysis using the Cox regression model, it was shown that hsa-miR-148a-3p is the most promising prognostic marker in CRPC based on liquid biopsy.

hsa-miR-148a-3p is one of the most highly expressed miRNAs in PCa tissues, as well as the most dominant in PCa metastasis [41]. Various studies have shown that high-grade tumors exhibit reduced levels of hsa-miR-148a-3p expression. It has also been shown that hsa-miR-148a-3p expression is downregulated in docetaxel-resistant variants of PCa cell lines, including PC-3 and DU145, and that hsa-miR-148a-3p is downregulated in PCa with a risk of biochemical recurrence. In addition, it has been shown that this tumor-suppressing miRNA can be downregulated in CRPC, which has been shown in PC3 cell culture leading to cancer progression and resistance to androgen deprivation therapy [42]. Based on our data on profiling exosomal miRNAs in the blood plasma of patients with CRPC during therapy, it was also shown that the differential expression of hsa-miR-148a-3p statistically significantly decreases with the progression of CRPC and is characterized by a strong correlation ( $\text{LogFC} = -2.49$ ;  $r_s = -0.75$ ).

In addition, a strong relationship was shown between the expression of this miRNA and a high risk of CRPC progression during therapy ( $\text{HR} = 2.05$ ;  $p < 0.005$ ). The results of statistically significant expression of hsa-miR-148a-3p with an increase in PSA levels during CRPC therapy were also confirmed by qPCR ( $p(W) = 0.02$ ).

Based on our results, as well as various literature data, a significant role of hsa-miR-148a-3p in the progression of CRPC is emphasized, which requires further study on an expanded sample with additional validation methods.

## 5. Conclusions

Thus, we obtained data on exosomal miRNA profiling during therapy in patients with metastatic CRPC. Signaling pathways associated with increased PSA levels during therapy have been identified, which contributes to the un-

derstanding of the molecular events underlying tumor progression in CRPC at the transcriptomic level. The identified signaling pathways and miRNAs with significant and specific expression, especially hsa-miR-148a-3p, can be further considered as new therapeutic targets and additional informative markers for assessing the aggressiveness of the tumor process.

## Abbreviations

PCa, prostate cancer; CRPC, castration-resistant prostate cancer; PSA, prostate specific antigen; NGS, next generation sequencing; TMM, Trimmed Mean of M-values; CPM, counts per million; QLF test, quasi-likelihood F-test; W test, Wilcoxon test;  $r_s$ , Spearman's rank correlation coefficient; qPCR, quantitative polymerase chain reaction; LogFC, binary logarithm of expression level ratio between groups; DE, differential expression.

## Author Contributions

AVK, KMN, BYA conceived and designed the work; EAP, IVK, MSF, ZGG, VSP, MVS performed the experiments; GSK, EAP, AAKo, AAKu analyzed the data; EAP, GSK and AVS wrote the manuscript. All authors read and approved the final manuscript.

## Ethics Approval and Consent to Participate

The study was approved by The Ethics committee of P.A. Herten Moscow Oncology Research Center, Ministry of Health of the Russian Federation. The study was done in accordance with the principles outlined in the Declaration of Helsinki (1964). All patients gave their informed consent for participation in the study.

## Acknowledgment

The authors thank the National Medical Research Radiological Center for providing the samples and their characterization. This work was performed using the equipment of the EIMB RAS "Genome" center ([http://www.eimb.ru/rus/ckp/ccu\\_genome\\_c.php](http://www.eimb.ru/rus/ckp/ccu_genome_c.php)).

## Funding

This work was financially supported by the Russian Science Foundation, grant 22-24-01093. The funding body played no role in the design of the study and collection, analysis, and interpretation of data and in writing the manuscript.

## Conflict of Interest

The authors declare no conflict of interest.

## References

- [1] Perner CH, Ebot EM, Wilson KM, Mucci LA. The Epidemiology of Prostate Cancer. *Cold Spring Harbor Perspectives in Medicine*. 2018; 8: a030361.
- [2] Cornford P, Bellmunt J, Bolla M, Briers E, De Santis M, Gross T, *et al*. EAU-ESTRO-SIOG Guidelines on Prostate Cancer. Part II: Treatment of Relapsing, Metastatic, and Castration-Resistant Prostate Cancer. *European Urology*. 2017; 71: 630–642.
- [3] Nikolaou M, Pavlopoulou A, Georgakilas AG, Kyrodimos E. The challenge of drug resistance in cancer treatment: a current overview. *Clinical Experimental Metastasis*. 2018; 35: 309–318.
- [4] Lippert TH, Ruoff HJ, Volm M. Intrinsic and acquired drug resistance in malignant tumors. The main reason for therapeutic failure. *Arzneimittelforschung*. 2008; 58: 261–264.
- [5] Lopez-Guerrero JA, Pastor-Navarro B, Claramunt-Alonso R, Garcia-Flores M, Rubio-Briones J. Liquid biopsy: possibilities and limitations in uro-oncology. *Archivos Espanoles de Urologia*. 2022; 75: 203–214.
- [6] Piñero-Pérez R, Abal M, Muñelo-Romay L. Liquid Biopsy for Monitoring EC Patients: Towards Personalized Treatment. *Cancers*. 2022; 14: 1405.
- [7] Raza A, Khan AQ, Inchakalody VP, Mestiri S, Yoosuf ZSKM, Bedhafi T, *et al*. Dynamic liquid biopsy components as predictive and prognostic biomarkers in colorectal cancer. *Journal of Experimental Clinical Cancer Research*. 2022; 41: 99.
- [8] Kalluri R, LeBleu VS. The biology, function, and biomedical applications of exosomes. *Science*. 2020; 367: eaau6977.
- [9] Dou G, Tian R, Liu X, Yuan P, Ye Q, Liu J, *et al*. Chimeric apoptotic bodies functionalized with natural membrane and modular delivery system for inflammation modulation. *Science Advances*. 2020; 6: eaba2987.
- [10] Kalluri R. The biology and function of exosomes in cancer. *Journal of Clinical Investigation*. 2016; 126: 1208–1215.
- [11] Gowda R, Robertson BM, Iyer S, Barry J, Dinavahi SS, Robertson GP. The role of exosomes in metastasis and progression of melanoma. *Cancer Treatment Reviews*. 2020; 85: 101975.
- [12] Soung YH, Nguyen T, Cao H, Lee J, Chung J. Emerging roles of exosomes in cancer invasion and metastasis. *BMB Reports*. 2016; 49: 18–25.
- [13] Shi J, Ren Y, Zhen L, Qiu X. Exosomes from breast cancer cells stimulate proliferation and inhibit apoptosis of CD133+ cancer cells in vitro. *Molecular Medicine Reports*. 2015; 11: 405–409.
- [14] Ahmadi M, Rezaie J. Tumor cells derived-exosomes as angiogenic agents: possible therapeutic implications. *Journal of Translational Medicine*. 2020; 18: 249.
- [15] Bach D, Hong J, Park HJ, Lee SK. The role of exosomes and miRNAs in drug-resistance of cancer cells. *International Journal of Cancer*. 2017; 141: 220–230.
- [16] Wang X, Zhou Y, Ding K. Roles of exosomes in cancer chemotherapy resistance, progression, metastasis and immunity, and their clinical applications. *International Journal of Oncology*. 2021; 59: 44.
- [17] Li S, Yi M, Dong B, Jiao Y, Luo S, Wu K. The roles of exosomes in cancer drug resistance and its therapeutic application. *Clinical and Translational Medicine*. 2020; 10: e257.
- [18] Lin H, Castillo L, Mahon KL, Chiam K, Lee BY, Nguyen Q, *et al*. Circulating microRNAs are associated with docetaxel chemotherapy outcome in castration-resistant prostate cancer. *British Journal of Cancer*. 2014; 110: 2462–2471.
- [19] Guo T, Wang Y, Jia J, Mao X, Stankiewicz E, Scandura G, *et al*. The Identification of Plasma Exosomal miR-423-3p as a Potential Predictive Biomarker for Prostate Cancer Castration-Resistance Development by Plasma Exosomal miRNA Sequencing. *Frontiers in Cell and Developmental Biology*. 2020; 8: 602493.
- [20] Enderle D, Spiel A, Coticchia CM, Berghoff E, Mueller R, Schlumpberger M, *et al*. Characterization of RNA from Exosomes and Other Extracellular Vesicles Isolated by a Novel Spin Column-Based Method. *PLoS ONE*. 2015; 10: e0136133.

- [21] Babayan A, Neumann MHD, Herdean A, Shaffer JM, Janning M, Kobus F, *et al.* Multicenter Evaluation of Independent High-Throughput and RT-qPCR Technologies for the Development of Analytical Workflows for Circulating miRNA Analysis. *Cancers*. 2020; 12: 1166.
- [22] Lu Y, Baras AS, Halushka MK. MiRge 2.0 for comprehensive analysis of microRNA sequencing data. *BMC Bioinformatics*. 2018; 19: 275.
- [23] Liao Y, Smyth GK, Shi W. FeatureCounts: an efficient general purpose program for assigning sequence reads to genomic features. *Bioinformatics*. 2014; 30: 923–930.
- [24] Robinson MD, McCarthy DJ, Smyth GK. EdgeR: a Bioconductor package for differential expression analysis of digital gene expression data. *Bioinformatics*. 2010; 26: 139–140.
- [25] Vlachos IS, Zagganas K, Paraskevopoulou MD, Georgakilas G, Karagkouni D, Vergoulis T, *et al.* DIANA-miRPath v3.0: deciphering microRNA function with experimental support. *Nucleic Acids Research*. 2015; 43: W460–W466.
- [26] Pudova EA, Krasnov GS, Kobelyatskaya AA, Savvateeva MV, Fedorova MS, Pavlov VS, *et al.* Gene Expression Changes and Associated Pathways Involved in the Progression of Prostate Cancer Advanced Stages. *Frontiers in Genetics*. 2020; 11: 613162.
- [27] Steinbichler TB, Dudás J, Skvortsov S, Ganswindt U, Riechelmann H, Skvortsova I. Therapy resistance mediated by exosomes. *Molecular Cancer*. 2019; 18: 58.
- [28] Moroishi T, Hansen CG, Guan K. The emerging roles of YAP and TAZ in cancer. *Nature Reviews Cancer*. 2015; 15: 73–79.
- [29] Moya IM, Halder G. Hippo-YAP/TAZ signalling in organ regeneration and regenerative medicine. *Nature Reviews Molecular Cell Biology*. 2019; 20: 211–226.
- [30] Park JH, Shin JE, Park HW. The Role of Hippo Pathway in Cancer Stem Cell Biology. *Molecules and Cells*. 2018; 41: 83–92.
- [31] Totaro A, Panciera T, Piccolo S. YAP/TAZ upstream signals and downstream responses. *Nature Cell Biology*. 2018; 20: 888–899.
- [32] Chan SW, Lim CJ, Chong YF, Pobbati AV, Huang C, Hong W. Hippo pathway-independent restriction of TAZ and YAP by angiomin. *Journal of Biological Chemistry*. 2011; 286: 7018–7026.
- [33] Yu F, Zhao B, Guan K. Hippo pathway in organ size control, tissue homeostasis, and cancer. *Cell*. 2015; 163: 811–828.
- [34] Wanjala J, Taylor BS, Chapinski C, Hieronymus H, Wongvipat J, Chen Y, *et al.* Identifying actionable targets through integrative analyses of GEM model and human prostate cancer genomic profiling. *Molecular Cancer Therapeutics*. 2015; 14: 278–288.
- [35] Koo KM, Mainwaring PN, Tomlins SA, Trau M. Merging new-age biomarkers and nanodiagnostics for precision prostate cancer management. *Nature Reviews Urology*. 2019; 16: 302–317.
- [36] Siegel PM, Massague J. Cytostatic and apoptotic actions of TGF-beta in homeostasis and cancer. *Nature Reviews Cancer*. 2003; 3: 807–821.
- [37] Barron DA, Rowley DR. The reactive stroma microenvironment and prostate cancer progression. *Endocrine-Related Cancer*. 2012; 19: R187–R204.
- [38] Bhowmick NA, Chytil A, Plieth D, Gorska AE, Dumont N, Shappell S, *et al.* TGF-beta signaling in fibroblasts modulates the oncogenic potential of adjacent epithelia. *Science*. 2004; 303: 848–851.
- [39] Bradner JE, Hnisz D, Young RA. Transcriptional addiction in cancer. *Cell*. 2017; 168: 629–643.
- [40] Li F, Mahato RI. MicroRNAs and drug resistance in prostate cancers. *Molecular Pharmaceutics*. 2014; 11: 2539–2552.
- [41] Watahiki A, Wang Y, Morris J, Dennis K, O'Dwyer HM, Gleave M, *et al.* MicroRNAs associated with metastatic prostate cancer. *PLoS ONE*. 2011; 6: e24950.
- [42] Fujita Y, Kojima K, Ohhashi R, Hamada N, Nozawa Y, Kitamoto A, *et al.* MiR-148a Attenuates Paclitaxel Resistance of Hormone-refractory, Drug-resistant Prostate Cancer PC3 Cells by Regulating MSK1 Expression. *Journal of Biological Chemistry*. 2010; 285: 19076–19084.